Journal of Quality Measurement and Analysis
e-ISSN: 2600-8602
https://doi.org/10.17576/jqma.2103.2025.09

JQMA 21(3) 2025, 151-159
http://www.ukm.my/jqma

STRESS INTENSITY FACTOR FOR A CURVILINEAR EDGE CRACK IN BONDED PLANES SUBJECTED TO TEAR STRESS

(*Faktor Keamatan Regangan untuk Retak Pinggir Lengkung dalam Satah Bercantum di Bawah Regangan Koyakan*)

NUR HAZIRAH HUSIN, NIK MOHD ASRI NIK LONG*, NORAZAK SENU & KHAIRUM HAMZAH

ABSTRACT

The singular integral equation (SIE) for a curvilinear edge crack that emerges at the interface of bonded planes under tear stress is formulated by making use of the modified complex potential (MCP) and the continuity conditions of displacement and traction. In the formulation of SIE, the unknown is the dislocation distribution function, while traction serves as the right-hand term. The obtained SIE is solved numerically by a semi-open quadrature rule. Numerical results are presented graphically to demonstrate the behaviour of dimensionless stress intensity factors (SIFs) for Modes I and II with different edge crack configurations and elastic constant ratios.

Keywords: edge crack; singular integral equation; bonded planes; modified complex potentials; stress intensity factor

ABSTRAK

Persamaan kamiran singular (PKS) untuk retak pinggir lengkung yang muncul pada permukaan antara dua satah yang bercantum di bawah regangan koyakan dirumuskan dengan menggunakan keupayaan kompleks terubahsuai (KKT) dan syarat kesinambungan sesaran serta daya tarikan. Dalam perumusan PKS, fungsi taburan sesaran yang tidak diketahui digunakan, manakala daya tarikan berfungsi sebagai terma di sebelah kanan. PKS yang diperoleh diselesaikan secara berangka menggunakan kaedah kuadratur separa terbuka. Keputusan berangka dibentangkan secara grafik untuk menunjukkan tingkah laku faktor keamatan regangan (FKR) tidak berdimensi bagi Mod I dan II dengan konfigurasi retak pinggir dan nisbah pemalar keanjalan yang berbeza.

Kata kunci: retak pinggir; persamaan kamiran singular; satah bercantum; keupayaan kompleks terubahsuai; faktor keamatan regangan

1. Introduction

The existence of cracks or flaws may affect the strength of materials and reduce the architectural structures' lifespan. Crack detection is vital for understanding how structures perform and remain safe, providing engineers and scientists with essential insights to improve durability and reliability under challenging conditions. Furthermore, analysing the stress intensity factor (SIF) is crucial for predicting structural stability and preventing potentially catastrophic failures (Fan *et al.* 2025). A number of researchers have carried out investigations on the behaviour of SIF in many types of cracks.

The analysis of SIF was performed by Choi (2016) for the problem related to two parallel edge cracks in bonded, distinct, homogeneous materials involving a functionally graded interlayer. For the thermal SIF, four edge cracks emerging through a square hole in piezoelectric materials were examined by Singh *et al.* (2018). Oda *et al.* (2023) evaluated the thermal SIF for an interfacial edge crack in a large two-material surface undergoing constant temperature. The findings indicated that SIF was affected by the single stress field, which includes a fixed term

and occurs when two material plates meet in the absence of a crack. The effect of the degree of bending on the SIF for a single edge crack was investigated by Azeez *et al.* (2023). Meanwhile, Pidgurskyi *et al.* (2024) studied the SIF for edge cracks under a bending moment using the finite element method. The extended finite element method was used by Lal *et al.* (2024) to analyse the mixed-mode SIF for an edge crack with varying material distributions. Hasebe (2021) discussed the dimensionless SIFs for Modes I and II of an obliquely edged crack in an orthogonal elastic half-plane.

A technique to evaluate the SIFs for the problem of kinked cracks was presented by Li *et al.* (2018). It was based on an estimation expression that developed via the stress field series at the initial crack end to a second order by making use of the weight function. For the inclined kinked edge crack in the semi-plane, Beghini *et al.* (2012) investigated Modes I and II SIFs under bi-axial stresses. Recently, the mechanical properties of a kinked crack have become crucial in engineering for the purposes of safety management and the development of crack networks. Current theories for kinked cracks depended on the perturbation approach, which was suitable for analysing tiny kinks, and SIFs were applicable in the closest area of the major crack tip (Liu & Wei 2021). A numerical simulation was applied to examine the SIF of an inclined edge crack in the interior plate vessel with pressure (Subbaiah & Bollineni 2020). Meanwhile, for arbitrary branched cracks, Liu & Wei (2023) proposed a semi-analytical solution on SIFs. The dimensionless SIFs for the problem of multiple circular arc cracks (Hamzah *et al.* 2019; Husin *et al.* 2021) were investigated as well.

This paper aims to (i) formulate a curvilinear edge crack emerging at the interface of bonded planes under tear stress and (ii) analyse the behaviour of the dimensionless SIFs at the crack tip for each crack configuration. Graphical representations of Modes I and II SIFs at the crack tip are provided to illustrate the relationship between the elastic constant ratios, crack opening angle, and the amplitude of the sine-like edge crack. The mathematical formulation of SIE is derived in Section 2, followed by the numerical examples in Section 3, and lastly, Section 4 is the conclusion.

2. Mathematical Formulation

Let $\phi'(\zeta) = \Phi(\zeta)$ and $\psi'(\zeta) = \Psi(\zeta)$ where $\Phi(\zeta), \Psi(\zeta)$ are the complex potentials functions associated with the resultant force functions (χ, γ), displacements (ω, z), and stresses $(\tau_x, \tau_y, \tau_{xy})$ as (Muskhelishvili 1977)

$$\begin{aligned} \tau_x + \tau_y &= 4Re\phi'(\zeta) && (1)\\ \tau_y - \tau_x + 2i\tau_{xy} &= 2[\bar{\zeta}\Phi'(\zeta) + \Psi(\zeta)] && (2)\\ -\gamma + i\chi &= \phi(\zeta) + \zeta\overline{\phi'(\zeta)} + \overline{\psi(\zeta)} && (3)\\ 2G(\omega + iz) &= \kappa\phi(\zeta) - \zeta\overline{\phi'(\zeta)} - \overline{\psi(\zeta)}. && (4) \end{aligned}$$

Eq. (4) exhibits the shear modulus of elasticity, denoted as G. For the plane stress and strain problems, $\kappa = (3 - z)/(1 + z)$ is used, and $\kappa = 3 - 4z$ is used. z abbreviates the Poisson's ratio, while $\bar{A}$ symbolises the conjugated value of A. Taking the derivative of (3) with respect to ζ results in

$$J\left(\zeta, \bar{\zeta}, \frac{d\bar{\zeta}}{d\zeta}\right) = \frac{d}{d\zeta}(-\gamma + i\chi) = \phi'(\zeta) + \overline{\phi'(\zeta)} + \frac{d\bar{\zeta}}{d\zeta}(\zeta\overline{\phi''(\zeta)} + \overline{\psi'(\zeta)}) = N + iT. \quad (5)$$

N and T in Eq. (5) represent the normal and tangential known functions of the tractions, respectively.

The problem of a half-plane with a crack is addressed using the modified complex potentials

(MCP) method. The principal and complementary components of MCP are as follows

$$\phi(\zeta) = \phi_p(\zeta) + \phi_c(\zeta) \tag{6}$$
$$\psi(\zeta) = \psi_p(\zeta) + \psi_c(\zeta). \tag{7}$$

The principal component can be derived through $g'(t)$, the crack dislocation distribution in an infinite plane. At the interface of the half-plane, the complementary component simultaneously eliminates the traction from its principal part. Following are the principal and complementary components' of complex potentials

$$\phi_p'(\zeta) = \frac{1}{2\pi}\int_L \frac{g'(t)dt}{t-\zeta} \tag{8}$$
$$\psi_p'(\zeta) = \frac{1}{2\pi}\int_L \frac{\overline{g'(t)}\,\overline{dt}}{t-\zeta} - \frac{1}{2\pi}\int_L \frac{\bar{t}g'(t)dt}{(t-\zeta)^2} \tag{9}$$
$$\phi_c'(\zeta) = -\overline{\phi_p'}(\zeta) - \overline{\psi_p}(\zeta) - \zeta\bar{\phi''}_p(\zeta) \tag{10}$$
$$\psi_c'(\zeta) = \overline{\psi_p}(\zeta) + 3\zeta\bar{\phi''}_p(z) + \zeta\bar{\psi''}_p(\zeta) + \zeta^2\bar{\phi'''}_p(\zeta) \tag{11}$$

where

$$g'(t) = -\frac{2Gi}{\kappa+1}\frac{d[(\omega(t)+iz(t))^+ - (\omega(t)+iz(t))^-]}{dt}, \quad t \in L. \tag{12}$$

The variable L represents the configuration of the crack. The $+$ and $-$ signs, respectively, indicate the upper and lower surfaces of the crack.

For an edge crack problem, as given in Chen & Hasebe (1995), the following equations yield

$$\phi_p'(\zeta) = \frac{e^{i\alpha}}{2\pi}\int_0^a \frac{g'(s)ds}{T_s-\zeta} \tag{13}$$
$$\psi_p'(\zeta) = \frac{e^{-i\alpha}}{2\pi}\int_0^a \frac{\overline{g'(s)}ds}{T_s-\zeta} - \frac{e^{i\alpha}}{2\pi}\int_0^a \frac{\bar{T}_s g'(s)ds}{(T_s-\zeta)^2} \tag{14}$$

where t is replaced with T_s, where $T_s = e + se^{i\alpha}$, and dt has been expressed as $e^{i\alpha}ds$, as applied directly in Eqs. (8) and (9).

Letting an edge crack originates at the interface of bonded planes towards the upper plane, the MCP presents as (Hamzah *et al.* 2021)

$$\phi_1(\zeta) = \phi_{1p}(\zeta) + \phi_{1c}(\zeta) \tag{15}$$
$$\psi_1(\zeta) = \psi_{1p}(\zeta) + \psi_{1c}(\zeta). \tag{16}$$

Conversely, ϕ_2 and ψ_2 represent the lower half plane. The conditions for continuity for Eq. (3) and Eq. (4) are expressed in the following manner, respectively

$$\left[\phi_1(\zeta) + \zeta\overline{\phi_1'(\zeta)} + \overline{\psi_1(\zeta)}\right]^+ = \left[\phi_2(\zeta) + \zeta\overline{\phi_2'(\zeta)} + \overline{\psi_2(\zeta)}\right]^-, \qquad T_s \in L \tag{17}$$
$$G_2\left[\kappa_1\phi_1(\zeta) - \zeta\overline{\phi_1'(\zeta)} - \overline{\psi_1(\zeta)}\right]^+ = G_1\left[\kappa_2\phi_2(\zeta) - \zeta\overline{\phi_2'(\zeta)} - \overline{\psi_2(\zeta)}\right]^-, \quad T_s \in L. \tag{18}$$

By using Eqs. (15) as well as (16) into Eqs. (17) and (18), the corresponding expressions are obtainable

$$\phi_{1c}(\zeta) = \lambda_1\left[\zeta\overline{\phi_{1p}'}(\zeta) + \overline{\psi_{1p}}(\zeta)\right] \tag{19}$$

$$\psi_{1c}(\zeta) = \lambda_2\overline{\phi_{1p}}(\zeta) - \lambda_1\left[\zeta\overline{\phi'_{1p}}(\zeta) + \zeta^2\overline{\phi''_{1p}}(\zeta) + \zeta\overline{\psi'_{1p}}(\zeta)\right] \tag{20}$$

$$\phi_2(\zeta) = (1+\lambda_2)\phi_{1p}(\zeta) \tag{21}$$

$$\psi_2(\zeta) = (1+\lambda_1)\psi_{1p}(\zeta) + (\lambda_1-\lambda_2)(\zeta\phi'_{1p}(\zeta)) \tag{22}$$

where

$$\lambda_1 = \frac{G_2 - G_1}{G_1 + \kappa_1 G_2}, \qquad \lambda_2 = \frac{\kappa_1 G_2 - \kappa_2 G_1}{G_2 + \kappa_2 G_1}. \tag{23}$$

λ_1 and λ_2 are the bimaterial elasticity parameters. $[N(s_0)+iT(s_0)]_{1p}$ and $[N(s_0)+iT(s_0)]_{1c}$ represent two fundamental components in the formulation of SIE of an edge crack in bonded planes.

By taking into account Eqs. (13) and (14) into Eq. (5), and allowing s to approach s_0, the principal part of traction is obtainable as follows

$$\begin{aligned}[N(s_0)+iT(s_0)]_{1p} &= \frac{1}{\pi}\int_0^a \frac{g'(s)ds}{s-s_0} + \frac{1}{\pi}\int_0^a C_1(s,s_0)\, g'(s)ds \\ &+ \frac{1}{\pi}\int_0^a C_2(s,s_0)\,\overline{g'(s)}ds \end{aligned} \tag{24}$$

where

$$\begin{aligned} C_1(s,s_0) =& \frac{e^{i\alpha}}{2}\left(\frac{1}{T_s - T_{s0}} + e^{-2i\alpha}\frac{1}{\bar{T}_s - \bar{T}_{s0}}\right) \\ C_2(s,s_0) =& \frac{e^{-i\alpha}}{2}\left(\frac{1}{\bar{T}_s - \bar{T}_{s0}} - e^{-2i\alpha}\frac{T_s - T_{s0}}{(\bar{T}_s - \bar{T}_{s0})^2}\right). \end{aligned}$$

Applying Eqs. (19) and (20) into Eq. (5), then utilising Eqs. (13) and (14), allowing s to approach s_0, results in the corresponding expression for the complementary part,

$$\begin{aligned}[N(s_0)+iT(s_0)]_{1c} &= \frac{1}{\pi}\int_0^a \frac{g'(s)ds}{s-s_0} + \frac{1}{\pi}\int_0^a \Big(D_1(s,s_0) + D_2(s,s_0)\Big)\, g'(s)ds \\ &+ \frac{1}{\pi}\int_0^a \Big(D_3(s,s_0) + D_4(s,s_0)\Big)\,\overline{g'(s)}ds \end{aligned} \tag{25}$$

where

$$\begin{aligned} D_1(s,s_0) =& \frac{e^{i\alpha}}{2}\left\{\lambda_1\left[\frac{1}{\bar{T}_s - T_{s0}} + \frac{1}{T_s - \bar{T}_{s0}} + \frac{\bar{T}_{s0} - \bar{T}_s}{(T_s - \bar{T}_{s0})^2}\right]\right\} \\ D_2(s,s_0) =& \frac{e^{i\alpha}}{2}\left\{e^{-2i\alpha}\left[\lambda_1\left(-\frac{1}{T_s - \bar{T}_{s0}} + \frac{\bar{T}_s - 3\bar{T}_{s0}}{(T_s - \bar{T}_{s0})^2}\right.\right.\right. \\ &\left.\left.\left. + \frac{2T_{s0}(T_s - \bar{T}_{s0})}{(T_s - \bar{T}_{s0})^3} + \frac{2\bar{T}_{s0}(\bar{T}_s - \bar{T}_{s0})}{(T_s - \bar{T}_{s0})^3}\right) + \lambda_2\left(\frac{1}{T_s - \bar{T}_{s0}}\right)\right]\right\} \\ D_3(s,s_0) =& \frac{e^{-i\alpha}}{2}\left\{\lambda_1\left[\frac{1}{\bar{T}_s - T_{s0}} + \frac{T_{s0} - \bar{T}_s}{(\bar{T}_s - T_{s0})^2} + \frac{1}{T_s - \bar{T}_{s0}}\right]\right\} \\ D_4(s,s_0) =& \frac{e^{-i\alpha}}{2}\left\{e^{-2i\alpha}\left[\lambda_1\left(\frac{T_{s0} - \bar{T}_{s0}}{(T_s - \bar{T}_{s0})^2} - \frac{1}{T_s - \bar{T}_{s0}}\right)\right]\right\}. \end{aligned}$$

Adding up Eqs. (24) and (25), the SIE for an edge crack originating from the boundary between

bonded planes towards the upper plane attainable as

$$\begin{aligned} N(s_0)+iT(s_0) &= \frac{1}{\pi}\fint_0^a \frac{g'(s)ds}{s-s_0}+\frac{1}{\pi}\int_0^a \mu_1(s,s_0)\, g'(s)ds \\ &\quad +\frac{1}{\pi}\int_0^a \mu_2(s,s_0)\,\overline{g'(s)}ds \end{aligned} \tag{26}$$

where

$$\begin{aligned} \mu_1(s,s_0) &= C_1(s,s_0)+D_1(s,s_0)+D_2(s,s_0) \\ \mu_2(s,s_0) &= C_2(s,s_0)+D_3(s,s_0)+D_4(s,s_0). \end{aligned}$$

The edge crack is represented on the real axis, utilising the curved length coordinate within the range given [0, a]. The dislocation distribution has a singularity at the specific crack's tip. Hence, Eq. (26) is modified with the corresponding representation

$$g'(s)=\sqrt{\frac{s}{(a-s)}}G(s). \tag{27}$$

On the right-hand side of Eq. (26), the singular integral is identified by the symbol $\fint$ in the first term, whilst the remaining terms can be described as regular integrals. The semi-open quadrature rules will be used for the singular and regular integrals, correspondingly (Boiko & Karpenko 1981)

$$\fint_0^a \frac{G(s)}{s-s_n}\sqrt{\left(\frac{s}{a-s}\right)}ds = \sum_{m=1}^{M}\frac{W_m G(s_m)}{s_m-s_n} \tag{28}$$

$$\int_0^a K(s,s_n)\sqrt{\left(\frac{s}{a-s}\right)}ds = \sum_{m=1}^{M} W_m K(s_m,s_n) \tag{29}$$

where

$$\begin{aligned} W_m &= \frac{a\pi}{M}\sin^2\frac{m\pi}{2M} && (m=1,2,\ldots,M-1), \\ s_m &= a\sin^2\frac{m\pi}{2M} && (m=1,2,\ldots,M), \\ s_n &= a\sin^2\frac{(n-0.5)\pi}{2M} && (n=1,2,\ldots,M). \end{aligned}$$

3. Numerical Examples

Calculating SIFs at the crack end is as follows

$$\begin{aligned} (K_1-iK_2) &= -\sqrt{2\pi}\lim_{s\to a}\sqrt{a-s}\; g'(s) \\ &= -\sqrt{2\pi a}\; G(a). \end{aligned} \tag{30}$$

Consequently, it implies

$$\begin{aligned} K_1 &= F_1(\alpha)p\sqrt{\pi a}, \quad F_1=-\sqrt{2}G(a) \\ K_2 &= -F_2(\alpha)p\sqrt{\pi a}, \quad F_2=-\sqrt{2}G(a). \end{aligned} \tag{31}$$

F_1 and F_2 correspond to the dimensionless SIFs Modes I and II, accordingly, at the crack end.

When the value of G_2 is zero, Eq. (26) can be simplified to represent a half-plane with the presence of an edge crack. Table 1 demonstrates that our computational findings for an edge crack align with those conclusions reported by Chen & Hasebe (1995). In the calculation, $M = 90$ was used.

Table 1: The dimensionless SIFs for an inclined edge crack versus α.

α(degree)	10	20	30	40	50	60	70	80	90
$f_1(\alpha)^{\text{a}}$	0.1494	0.3057	0.4631	0.6250	0.7816	0.9204	1.0286	1.0978	1.1216
$f_1(\alpha)^{\text{b}}$	0.1495	0.3058	0.4633	0.6252	0.7814	0.9208	1.0289	1.0985	1.1219
$f_2(\alpha)^{\text{c}}$	0.1849	0.2709	0.3358	0.3648	0.3544	0.3057	0.2243	0.1186	0.0000
$f_2(\alpha)^{\text{d}}$	0.1851	0.2709	0.3359	0.3646	0.3547	0.3060	0.2244	0.1186	0.0000

[a] Present study, [b]Chen & Hasebe (1995)

Consider three different edge crack configurations in two bonded planes under tear stress $\tau_{xy_j} = p$, as displayed in Figure 1. R, α, and A are defined in Figure 1. In Figure 1b, an arc edge crack emerges at the positive x-axis in the upper half of two bonded planes. A sine-shaped edge crack emerges at $x = 0$ and extends towards $x = \pi/2$ in the upper part of two bonded planes, as illustrated in Figure 1c. The equation describing the sine-like edge crack is $y = \rho \sin(\beta x)$, where $0 \leq \beta x \leq \frac{\pi}{2}$ and ρ signifies the amplitude.

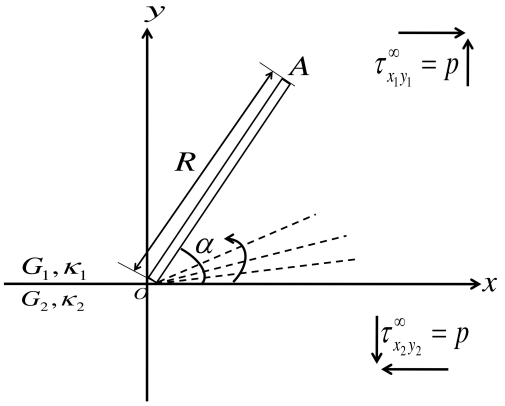

(a) An inclined edge crack

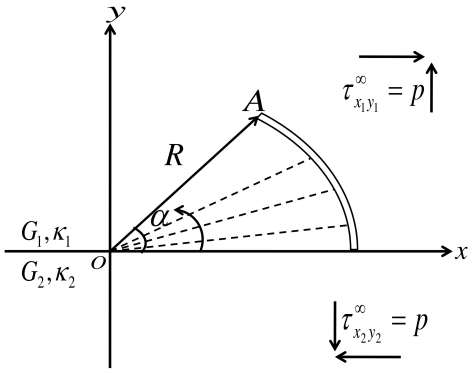

(b) An arc edge crack emerges at the positive x-axis

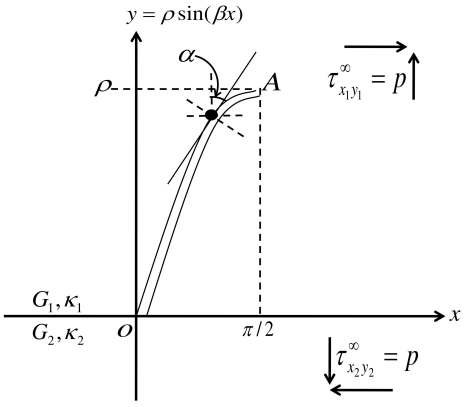

(c) A sine-like edge crack emerges at $x = 0$ towards $x = \pi/2$

Figure 1: Edge crack originating from the boundary between bonded planes under tear stress, $\tau_{xy_j} = p$.

Figure 2 displays the dimensionless SIFs for edge crack problems in Figures 1a, 1b and 1c. When $\alpha < 50^{\circ}$, F_1 decreases but increases when $\alpha > 50^{\circ}$ for all values of $G2/G1$ except for $G2/G1 = 0.0$, which is increases as α increases. This is due to the strong interaction between the crack tip and the plane's boundary. As $G2/G1$ increases, F_2 decreases when $\alpha < 60^{\circ}$, but F_2 increases when $\alpha > 60^{\circ}$. The inclination angle of the crack, α, in relation to the applied load influences the stress concentration variable, causing an increase or decrease in the SIF due to the combined effect of normal and shear stresses.

It is found that when α increases, F_1 decreases uniformly, but F_2 increases. When $\alpha > 75^{\circ}$, for $G2/G1 = 0.0$, F_2 increases exponentially. It is also observed that when a crack emerges at the negative x-axis, F_1 exhibits similar behaviour to its counterparts, where F_2 is negative of F_2. The symmetrical nature of the problem and the equal distribution of stress on the crack's faces lead to this effect. This analysis verifies the accuracy of our findings.

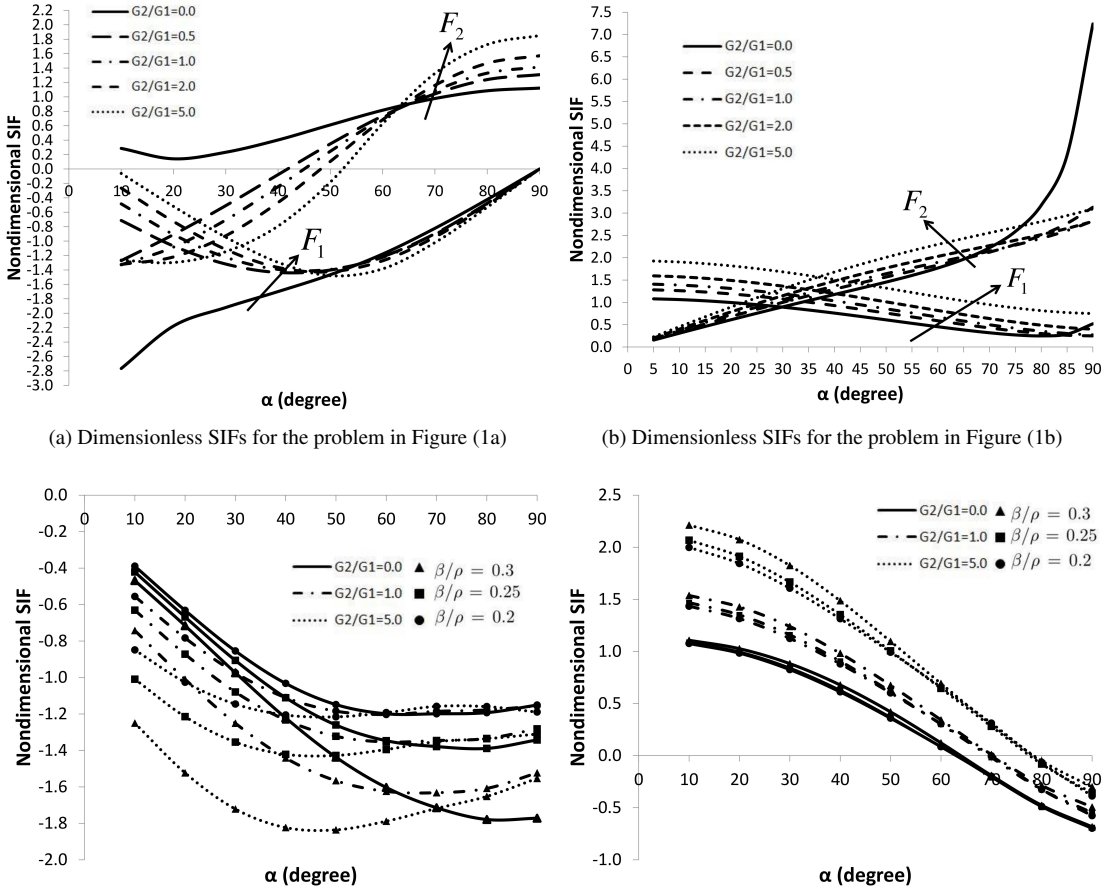

(a) Dimensionless SIFs for the problem in Figure (1a)

(b) Dimensionless SIFs for the problem in Figure (1b)

(c) Dimensionless SIF F_1 for the problem in Figure (1c)

(d) Dimensionless SIF F_2 for the problem in Figure (1c)

Figure 2: Dimensionless SIFs F_1 and F_2 for dissimilar edge crack configurations by varying the elastic constant ratios, $G2/G1$ and α.

The value of F_1 is observed to decrease when the ratio of β/ρ increases (see Figure 2c). β/ρ influences the SIF by altering the crack's geometry, affecting the stress concentration near the crack end. For $\alpha < 40^{\circ}$, as the ratio $G2/G1$ increases, F_1 decreases. Depending on the opening angle of the crack, α, the ratio $G2/G1$ affects the stress distribution near the crack end. For every value of β/ρ, the value of F_2 decreases as α increases. It is observed that the increased value of $G2/G1$ results in an increase in F_2 for every value of β/ρ (see Figure 2d).

4. Conclusion

In this paper, a curvilinear edge crack emerges at the interface of bonded planes subjected to tear stress and is formulated into SIE with the help of MCP. The semi-open quadrature rule is employed, and SIE is then solved numerically. As a conclusion, the behaviour of the dimensionless SIFs for Modes I and II at the crack end depends on the crack configuration and is strongly affected by the amplitude of the sine-like edge crack, the elastic constant ratios, and the crack opening angle.

Investigating the behaviour of the SIF at the crack end may help engineers construct stronger, safer infrastructure and components. Therefore, it protects human lives and reduces financial losses due to structural damages. Future research can concentrate on formulating multiple edge cracks originate at the interface of bonded planes, either (i) towards the upper plane or (ii) towards both the upper and lower planes.

Acknowledgement

The authors gratefully acknowledge Universiti Putra Malaysia for the funding provided via the Putra Grant, project number GP/2023/9752700.

References

Azeez A., Leidermark D. & Eriksson R. 2023. Stress intensity factor solution for single edge cracked tension specimen considering grips bending effects. *Procedia Struc. Integr.* **47**: 195–204.

Beghini M., Benedetti M., Fontanari V. & Monelli B.D. 2012. Stress intensity factors of inclined kinked edge cracks: A simplified approach. *Eng. Fract. Mech.* **81**: 120–129.

Boiko A.V. & Karpenko L.N. 1981. On some numerical methods for the solution of the plane elasticity problem for bodies with cracks by means of singular integral equations. *Int. J. Fract.* **17**: 381–388.

Chen Y.Z. & Hasebe N. 1995. Solution of multiple edge crack problem of elastic half-plane by using singular integral equation approach. *Commun. Numer. Methods Eng.* **11**(7): 607–617.

Choi H.J. 2016. Analysis of stress intensity factors for edge interfacial cracks in bonded dissimilar media with a functionally graded interlayer under antiplane deformation. *Theor. Appl. Fract. Mech.* **82**: 88–95.

Fan C., Ding Y., Liu X. & Yang K. 2025. A review of crack research in concrete structures based on data driven and intelligent algorithms. *Structures* **75**: 108800.

Hamzah K.B., Nik Long N.M.A., Senu N. & Eshkuvatov Z.K. 2019. Stress intensity factor for multiple cracks in bonded dissimilar materials using hypersingular integral equations. *Appl. Math. Model.* **73**: 95–108.

Hamzah K.B., Nik Long N.M.A., Senu N. & Eshkuvatov Z.K. 2021. A new system of singular integral equations for a curvilinear crack in bonded materials. *Journal of Physics: Conference Series* **1988**: 012003.

Hasebe N. 2021. Stress analysis for an orthotropic elastic half plane with an oblique edge crack and stress intensity factors. *Acta Mech.* **232**: 967–982.

Husin N.H., Nik Long N.M.A. & Senu N. 2021. Hypersingular integral equation for triple circular arc cracks in an elastic half-plane. *Malaysian J. Math. Sci.* **15**(3): 387–396.

Lal A., Kulkarni N.M., Singh S., Mahto A. & Kumar R. 2024. Mixed mode stress intensity factor analysis on edge cracked FGM plate with different material distribution models by XFEM. *J. Mech. Sci. Technol.* **38**: 6015–6029.

Li Y., Sun T., Gao Q. & Tan C. 2018. A stress intensity factor estimation method for kinked crack. *Eng. Fract. Mech.* **188**: 202–216.

Liu Z.E. & Wei Y. 2021. An analytical solution to the stress fields of kinked cracks. *J. Mech. Phys. Solids* **156**: 104619.

Liu Z.E. & Wei Y. 2023. A semi-analytical solution to the stress intensity factors of branched cracks. *J. Mech. Phys. Solids* **179**: 105351.

Muskhelishvili N.I. 1977. *Some Basic Problems of The Mathematical Theory of Elasticity*. Dordrecht, Netherlands: Springer.

Oda K., Shinmoto T. & Noda N.A. 2023. Thermal stress intensity factor of an edge interface crack under arbitrary material combination considering double singular stress fields before and after cracking. *Acta Mech.* **234**: 3037–3059.

Pidgurskyi M., Stashkiv M., Rohatynskyi R., Pidgurskyi I., Senchyshyn V. & Mushak A. 2024. Investigation of the stress intensity factor for the edge crack in I-beam under bending moment. *Procedia Struc. Integr.* **59**: 322–329.

Singh A., Das S. & Craciun E.M. 2018. Thermal stress intensity factor for an edge crack in orthotropic composite media. *Compos. B Eng.* **153**: 130–136.

Subbaiah A. & Bollineni R. 2020. Stress intensity factor of inclined internal edge crack in cylindrical pressure vessel. *J. Fail. Anal. Prev.* **20**: 1524–1533.

Institute for Mathematical Research
Universiti Putra Malaysia
43400 UPM Serdang
Selangor, MALAYSIA
E-mail: nurhazirah.husin@gmail.com

Department of Mathematics and Statistics
Faculty of Science
Universiti Putra Malaysia
43400 UPM Serdang
Selangor, MALAYSIA
E-mail: nmasri@upm.edu.my, norazak@upm.edu.my*

Faculty of Mechanical and Manufacturing Engineering Technology
Universiti Teknikal Malaysia Melaka
Hang Tuah Jaya
76100 Durian Tunggal
Melaka, MALAYSIA
E-mail: khairum@utem.edu.my

Received: 15 August 2024
Accepted: 20 April 2025

*Corresponding author